Improved femoral neck fracture predictions using anisotropic failure criteria models

Martine Pithioux, Patrick Chabrand, Christian Hochard, Pierre Champsaur

IMPROVED FEMORAL NECK FRACTURE PREDICTIONS USING ANISOTROPIC FAILURE CRITERIA MODELS

MARTINE PITHIOUX*, PATRICK CHABRAND*,‡, CHRISTIAN HOCHARD† and PIERRE CHAMPSAUR*

*Institute of Movement Science
UMR, University of the Mediterranean
CNRS, 13009 Marseille, France

†Laboratory of Mechanics and Acoustics,
UPR CNRS, 13009 Marseille, France

Finite element models are widely used to assess long bone strength, implant stability and other clinical problems. In most of the models presented so far in the literature, the bone is taken to be isotropic, and the occurrence of failure is predicted by defining a threshold von Mises stress. However, human bone is found to show orthotropic behavior. Studies so far have focused only on the use of anisotropic criteria in orthotropic models designed to predict the occurrence of human femur failure. The aim of this study was therefore to investigate how specific finite element models for human femora combined with composite failure theories could be used to improve failure predictions *in vitro*. For this purpose, nine human proximal femora were tested mechanically up to failure under the loading conditions present during the one-leg stance phase in walking. Specific finite element models using various materials to represent the bone were generated for each femur. First, the bone material was modeled in the form of an isotropic brittle material, and the von Mises criterion was used to predict the occurrence of fracture. Second, the bone was modeled as a transversely isotropic brittle material with asymmetric strength characteristics, and the occurrence of fracture was predicted using the Hill and the Tsai–Wu criteria. The results obtained here show that the transversely isotropic model combined with Tsai–Wu and Hill criteria accurately predicted the fracture load (values of $R^2 = 0.94$ and SEE = 10.3% were obtained with the Tsai–Wu criteria and $R^2 = 0.82$ and SEE = 22.9% were obtained with the Hill criteria), while the isotropic model combined with the von Mises criterion overestimated the fracture load, although a good correlation was generally observed with the experimental results ($R^2 = 0.77$, SEE = 30.6%).

Keywords: Femoral neck fractures; failure criteria; finite element analysis; experimental tests; transversely isotropic material.

‡Corresponding author.

1. Introduction

While fall mechanics influence the outcome of each fall,[1–4] clinicians would clearly benefit from a method of assessing the strength of the proximal femur *in vivo* for individual patients. Finite element models are widely used to assess long bone strength, implant stability and other clinical problems.[5–9] Boundary conditions used in these models represent experimental conditions under one-leg stance phase in walking.[10–12] The accuracy of these models depends on their ability to describe the bone geometry and the mineralization processes involved. To improve the description of bone density and geometry, Computed Tomography (CT) scans were used to develop finite element models, taking into account the 3D bone structure and the distribution of the bone mineral.[1,6,7,13–22]

In most of the previous models, the bone was assumed to behave like an isotropic material and CT scans were used only to describe the bone structure and to calculate homogeneous mechanical properties.[5,19,23–27] The orthotropic behavior of bone was recently studied in order to determine the strength of the long bones.[13,14,28]

These models are mainly used to predict *in vitro* bone fracture, based on failure theories. The most frequently used models of this kind are those based on the von Mises criterion and the maximum principal stress criterion,[23,25,29,30] where the bone is assumed to have isotropic behavior. However, bone is known to be a brittle material with asymmetric strength characteristics.[14,31–33] To address this issue, various authors[30,34,35] attempted to develop models based on isotropic bone material properties and anisotropic failure criteria established in the case of brittle composite materials: However, this approach did not improve the failure predictions in comparison with models based on the classical criteria. Few attempts have been made so far to use anisotropic criteria to predict failure in orthotropic models for human bone. The aim of this study was therefore to investigate how sophisticated finite element models combined with appropriate failure theories accounting for the differences in the tension and compression strength characteristics of cortical bone can be used to improve failure predictions. For this purpose, a combined experimental and numerical study was performed.

Experimentally, nine human proximal femora were imaged using a CT device and tested mechanically up to failure. The CT scans of the tested femora were then used to generate specific finite element models. In these models, the bone is taken to be a composite material composed of cortical and cancellous bone. The cortical bone was modeled as a transversely isotropic brittle material with asymmetric strength characteristics. The cancellous bone was modeled in the form of an isotropic brittle material with symmetric strength characteristics. The failure loads occurring in the transversely isotropic models were calculated using the Hill and the Tsai–Wu criteria. These results were compared with those obtained with an isotropic numerical model in which the failure loads were determined on the basis of the von Mises criterion.

2. Material and Methods

2.1. *Preparation of the specimens*

Nine human proximal femora freshly collected from seven anonymous donors were obtained from the Pathological Anatomy Laboratory at La Timone Hospital, Marseille (France). The specimen did not show any anatomical signs of osteoarthritis in the cartilages or any deformity. The age of the donors ranged from 74 to 91 years, and averaged 85 years. Femora 1 and 2 and femora 7 and 8 came from the same donors. Prior to preparing the femora for the mechanical tests, CT scans were performed (scanner model: General Electric LightSpeed Pro16, 140 kV; Medical imagery department at La Timone Hospital, Marseilles). An axial scan protocol was adopted with a slice thickness of 0.625 mm and a pixel value of 0.225 mm. The specimens were frozen to $-20°$C and kept until the day before the test.

2.2. *Experimental tests*

All the experimental studies were realized in the Pathological Anatomy Laboratory at La Timone University. The experimental device was designed in order to load proximal femora in a physiological position. The load prescribed corresponded here to the tensor applied to the femoral head by the hip joint during monopodal stance. For this purpose, the 3D geometry of each femur was generated and used to determine the orientation of its anatomic axis (that of the shaft and neck axes) with a CAD software program, with respect to the vertical experimental compression loads.

Next, a threaded rod was introduced into the femur diaphysis, in order to check the frontal orientation and to improve the fixation of the femur in the device (see Fig. 1(a)). Each femur was then placed in the sagittal plane at the calculated inclination and held in place by a dead stop screw (see Fig. 1(a)). A sample holder was designed using a PVC sleeve, in which the proximal femur is placed and immersed in epoxy resin (type F12 Axson Technologies) under the intertrochanteric line. With this device, compression tests were performed in which the stress was concentrated in the trochanteric region of the proximal femur, under the target region (the neck of the femur). This device reduces the influence of the stress concentration on the femoral neck. All the femora were thawed out for 24 h in a moist atmosphere before being prepared and tested.

The proximal femora were tested mechanically up to failure under quasistatic conditions during controlled displacements (2 mm/min), using a compression machine equipped with load cell sensors (up to 2000 daN ± 0.25). The load was applied to the femoral head with an elastomer ring indenter so as to distribute the load as evenly as possible over the contact surface.[36] The fracture load (F_{exp}) was defined as the maximum load achieved.

The above device was designed and validated by performing numerical simulations, and an experimental test was also performed on two dry femora to check the validity of the results obtained.

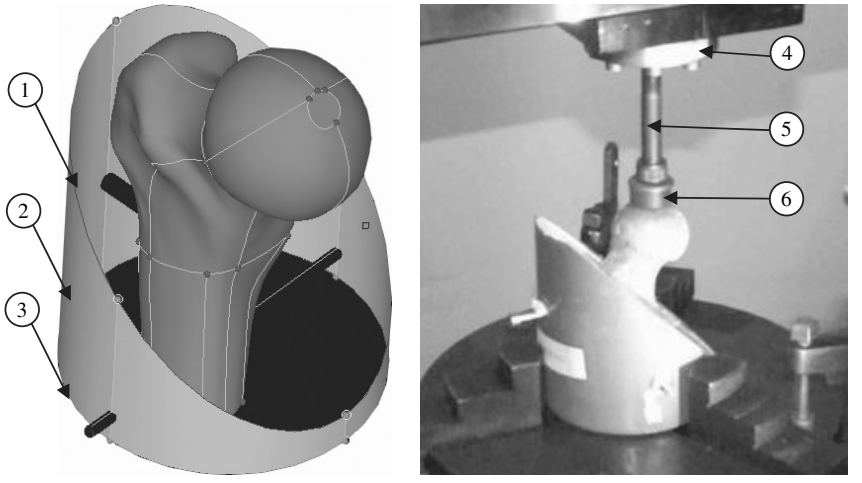

(a) (b)

Fig. 1. (a) 3D reconstruction of the fixation device holding the proximal femur: (1) screw, (2) PVC sleeve, (3) treaded rod. (b) Device in test machine: (4) load cell, (5) metallic indenter, (6) elastomer ring. An epoxy resin (AXON F1) was used to immerged specimen in PVC sleeve.

2.3. *Specific finite element models*

Numerical models were developed to simulate the experimental tests. Thus, the boundary conditions and load case applied in this model represents experimental conditions. Finite element models based on CT images were developed. A Voxel is the elementary volume used in tomography and Keyak developed a voxel method to represent the bone density geometrically. This method was used. Each elementary volume was used to generate one hexahedral H8 element. These H8 elements are complete integration elements which are suitable for studies involving traction-compression and shear loads.[37] The size of the elements used in the overall model averaged 0.6 mm. Viceconti shows that when the model has more than 10,000 elements there is only 2% of error. The models of the study included 100,000 elements. The normal direction of the transverse isotropic of cortical bone, in the proximal femur, was assumed to be the same as the femoral neck axis. Thus, the main axis of the model was adjusted within the femoral neck axis. So, the generated elements had an axis identical to the neck axis (Fig. 2).

In each voxel, the CT-scan bone mineral density was used to calculate the mechanical properties of the element generated (Table 1). The difference between the cortical and the porous bone is defined using a threshold of the effective density of $0.2\,\mathrm{g/cm^3}$.

First, an isotropic model is considered in which the whole bone was assumed to be an isotropic and brittle material with only one strength limit under both tension and compression loading conditions. The Young's modulus and strength limit of this

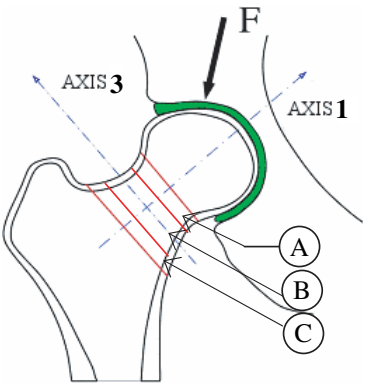

Fig. 2. Frontal view of proximal femur with applied load (F). (A) subcapital region of proximal femur. (B) cervical region of proximal femur. (C) trochanteric region of proximal femur.

Table 1. Elastic properties and failure stress of the kth element, in cortical and cancellous bone, defined in the transversely isotropic models.

Elastic modulus (MPa)	Failure stress limits (MPa)
Cortical bone	
$E_{1,k} = 14900 \times \rho_{\text{app},k}^{1,86}$	$\sigma_{1,k}^{C} = 102 \times \rho_{\text{app},k}^{1,86}$
$E_{2,k} = E_{3,k} = 0.6 \times E_{1,k}$	$\sigma_{2,k}^{C} = \sigma_{3,k}^{C} = 0.6 \times \sigma_{1,k}^{C}$
$G_{12,k} = G_{13,k} = 0.6 \times E_{1,k}$	$\sigma_{i,k}^{T} = 0.5 \times \sigma_{i,k}^{C}$
$\nu_{21} = \nu_{31} = 0.21;\ \nu_{23} = 0.42$	$\tau_{ij,k} = 0.25 \times \sigma_{i,k}^{C}$
Cancellous bone	
$E_k = 14900 \times \rho_{\text{app},k}^{1,86}$	$\sigma_k = 102 \times \rho_{\text{app},k}^{1,86}$
$\nu = 0.3$	

material were calculated from the bone mineral density using power laws described by Keyak *et al.*,[5] including both cortical and cancellous tissues (Eq. (1)).

$$E_k = 14900 \times \rho_{\text{app},k}^{1,86}; \quad \sigma_k = 102 \times \rho_{\text{app},k}^{1,86}. \tag{1}$$

Second, the two tissues involved were studied separately. The cancellous bone tissue was assumed to be an isotropic brittle material and the cortical bone was assumed to be a transversely isotropic[34] brittle material with asymmetric strength characteristics.[31,33,38,39] The isotropic transverse behavior was supposed to be used for elements with a Young modulus from 10 to 30 GPa and the isotropic behavior was used for elements with a Young modulus less than 10 GPa. The Young modulus in the main direction of isotropy of the bone was calculated from the apparent density using the power law described by Keyak *et al.*,[5] and its elastic properties were calculated in the other direction (E_i; G_{ij}), based on experimental findings and given *versus* the Young's modulus calculated in the principal direction

$(E_{i;k})$.[39–41] The cortical compression strength limit in the principal direction was calculated from the apparent density,[5] and its tension and shear strength limits in the principal and transversal directions were obtained empirically from the principal compression strength limit, based on previous experimental findings.[31,39] The equations describing the elastic properties and strength limits of the kth element in both cortical and cancellous parts are given in Table 1.

2.4. *Failure criteria*

The failure loads were predicted with both models using failure criteria and compared with experimental results. The failure load was defined as the calculated load under which the first element reaches a limit defined by a stress function. In this study, the von Mises criterion was used to calculate the failure load in the isotropic models, whereas the Hill and the Tsai–Wu criteria were used to calculate the failure load in the transversely isotropic models. The Hill criterion extends the use of von Mises failure criteria to orthotropic materials, and the Tsai–Wu criterion extends the use of the Hill criterion by taking into account the difference between the tension and compression behavior of cortical bone.[31,42] In the case of cancellous bone, both criteria were identical to von Mises criteria.

The general form of the von Mises criterion for the kth element in terms of the stress components (σ_{ij}^k) is

$$\begin{aligned} f(\sigma) = [0.5((\sigma_{yy}^k - \sigma_{xx}^k)^2 + (\sigma_{zz}^k - \sigma_{xx}^k)^2 + (\sigma_{yy}^k - \sigma_{zz}^k)^2) \\ + 3((\tau_{xy}^k)^2 + (\tau_{xz}^k)^2 + (\tau_{yz}^k)^2)]^{1/2}/\sigma_k. \end{aligned} \tag{2}$$

The general form of the Hill criterion for the kth element in terms of the stress components (σ_{ij}^k) is

$$\begin{aligned} f(\sigma) = [F((\sigma_{yy}^k - \sigma_{xx}^k)^2 + (\sigma_{zz}^k - \sigma_{xx}^k)^2) + H(\sigma_{yy}^k - \sigma_{zz}^k)^2 \\ + 2L((\tau_{xy}^k)^2 + (\tau_{xz}^k)^2) + 2N(\tau_{yz}^k)^2]^{1/2}, \end{aligned} \tag{3}$$

where F, H, L and N are coefficients calculated from the stress strength limits of this element.

$$\begin{gathered} 2F = 1/(\sigma_{1,k}^C)^2; \quad 2H = 2/(\sigma_{2,k}^C)^2 - 1/(\sigma_{1,k}^C)^2; \\ 2L = 1/(\sigma_{12,k})^2; \quad 2N = 1/(\sigma_{23,k})^2. \end{gathered} \tag{4}$$

The general form of the Tsai–Wu criterion for the kth element in terms of the stress components (σ_{ij}^k) is

$$\begin{aligned} f(\sigma) = [F_1\sigma_{xx}^k + F_2(\sigma_{yy}^k + \sigma_{zz}^k) + F_{11}(\sigma_{xx}^k)^2 + F_{22}((\sigma_{yy}^k)^2 + (\sigma_{zz}^k)^2) \\ + F_{66}(\tau_{yz}^k)^2 + F_{44}((\tau_{xy}^k)^2 + (\tau_{xz}^k)^2) + 2F_{12}(\sigma_{xx}^k\sigma_{yy}^k + \sigma_{xx}^k\sigma_{zz}^k) \\ + 2F_{23}\sigma_{yy}^k\sigma_{zz}^k]^{1/2}, \end{aligned} \tag{5}$$

where F_1, F_2, F_{11}, F_{22}, F_{44}, F_{66} are coefficients calculated from the stress strength limits of the kth element. F_{12} and F_{23} allow to consider the coupling effect. Due to

the fact that bone is considered as brittle material, this effect is negligible with an ultimate low strain.[42]

$$F_1 = 1/\sigma_{1,k}^T - 1/\sigma_{1,k}^C; \quad F_2 = 1/\sigma_{2,k}^T - 1/\sigma_{2,k}^C; \quad F_{11} = 1/(\sigma_{1,k}^T \sigma_{1,k}^C)$$
$$F_{22} = 1/(\sigma_{2,k}^T \sigma_{2,k}^C); \quad F_{44} = 1/\sigma_{12,k}^2; \quad F_{66} = 1/\sigma_{23,k}^2 \qquad (6)$$

The boundary conditions and the loading conditions constituted the experimental conditions. The load was applied to a restricted region of the femoral head, as occurs in mechanical tests.

The equations governing both models were solved using standard finite element methods (ABAQUS, Hibbitt, Karlsson and Sorensen, Inc.).

In order to assess the ability of the finite element models to predict fracture loads, simple linear regression analyzes were performed between the experimentally measured loads (F_{exp}) and the failure loads ($F_{\text{Tsai-Wu}}$, F_{Hill}, $F_{\text{von Mises}}$) predicted by the finite element models, and the percentage standard error of the estimated values (SEE) was calculated (standard error of the estimated fracture load $\times$ 100/mean estimated fracture load).

3. Results

Results from femora 1 and 2 and femora 7 and 8 were close to being identical which shows that the failure force is quite identical for same donors' femora.

The three main kinds of fractures observed corresponded to those frequently detected in clinical practice (Fig. 3). The fractures of the first type, which occurred in femora 1, 2 and 3, were initiated at the level of the subcapital section and

(a) (b) (c)

Fig. 3. Typical femoral neck fractures observed in mechanical testing. (a) Type 1: fractures initiated at subcapital section and showed a vertical bifurcation. (b) Type 2: subcapital fracture. (c) Type 3: fractures initiated at cervical section and showed a vertical bifurcation.

showed a vertical bifurcation (Fig. 3(a)). The fracture of the second type, which was observed in femur 4, was clearly a subcapital fracture (Fig. 3(b)). The fracture of the third type, which happened in the remaining femora, was initiated at cervical neck section level and showed a vertical bifurcation.

The first finite element in which the failure limit was reached as defined using the Tsai–Wu failure model criteria, was located in the subcapital section in the case of femora 1, 2 and 3, and in the cervical section of the femoral neck in the other femora; whereas on the basis of both the von Mises and Hill criteria, the first element to reach failure limit was located in the subcapital section of the femoral neck in the case of all the specimens.

The failure load values predicted by the finite element models and the experimental results are given in Fig. 4. Results showed that in the under capital section the shear stress is prevalent, whereas in the cervical section, the flexion is prevalent.

Figure 5 gives the correlations obtained between the failure loads predicted and the experimental results. The failure load calculated on the basis of all the three failure criteria were found to be significantly correlated with the experimental failure load values, but the best correlation was with the Tsai–Wu predictions ($R^2 = 0.77$ with the von Mises criteria, $R^2 = 0.82$ with Hill's criteria and $R^2 = 0.94$ with the Tsai–Wu criteria). The percentage standard error of the estimated values (SEE) was 30.6%, 22.9% and 10.3% with respectively the von Mises, Hill and Tsai–Wu model predictions.

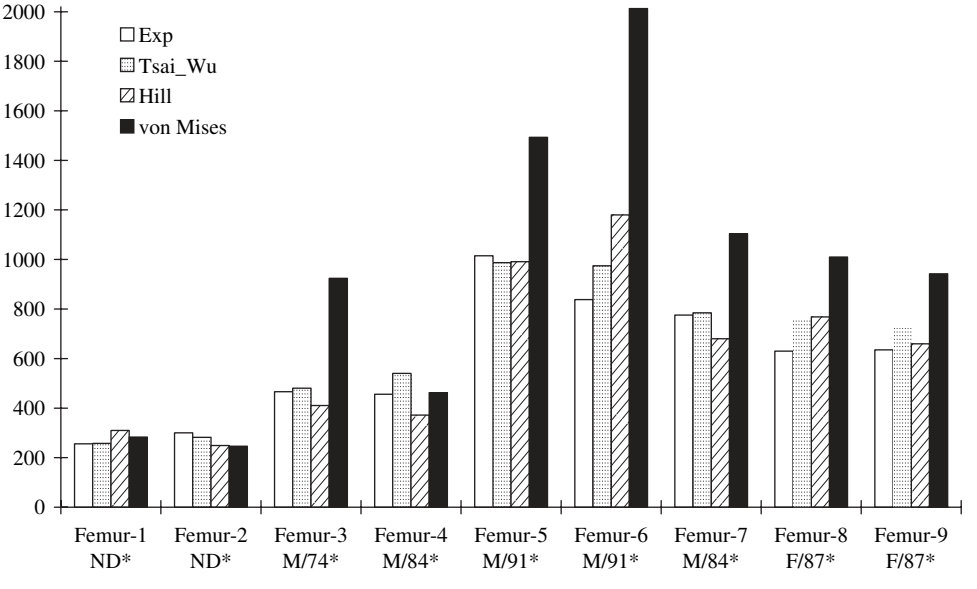

Fig. 4. Comparison of experimental measured fracture loads "F_{exp}" with predicted fracture loads obtained by Tsai–Wu criterion "$F_{\text{Tsai}-\text{Wu}}$," Hill criterion "$F_{\text{Hill}}$" and Von Mises criterion "$F_{\text{von Mises}}$." *Donor's gender and age (ND = not defined).

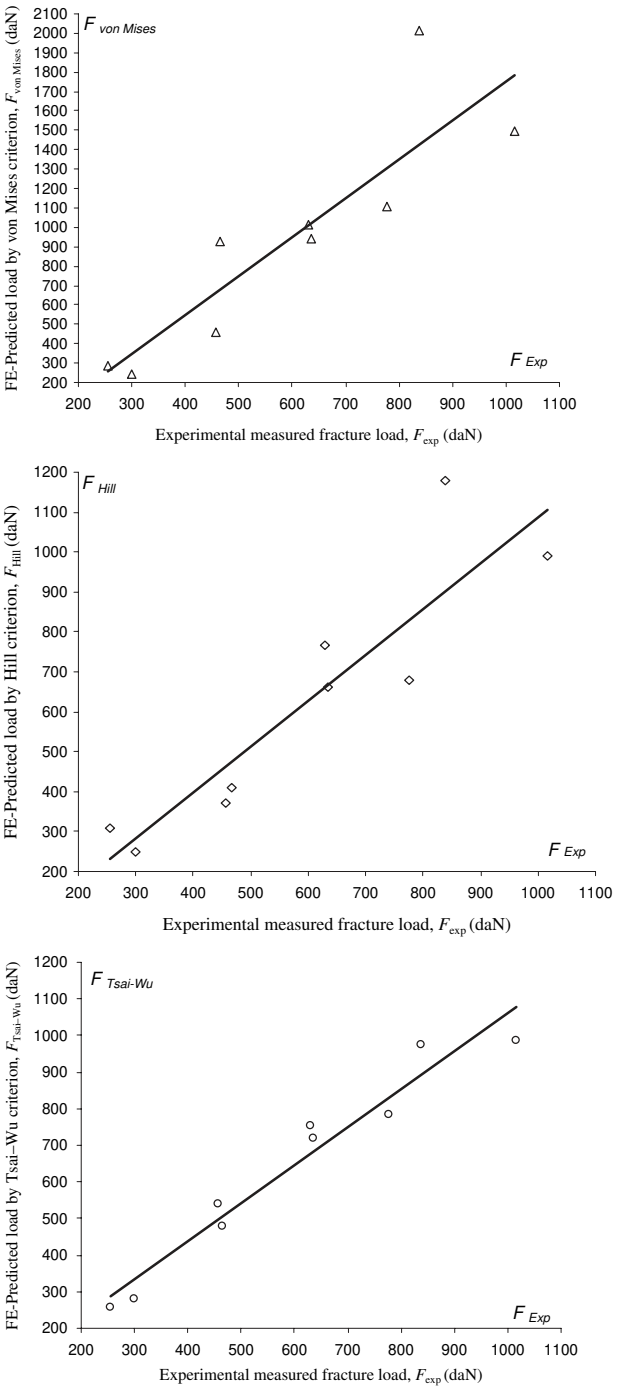

Fig. 5. Experimental measured fracture load versus finite element fracture load (daN) predicted using the von Mises criterion (Δ), Hill criterion (◇) and Tsai–Wu criterion (○).

In addition, when the femora sustained a cervical fracture, the von Mises criterion overestimated the failure load. This may be attributed to the fact that the shear stress is weaker in the cervical region (which is far from the loading area) than in the subcapital region (far from loading area).

4. Discussion

The present experiments were performed using an original device designed to prescribe vertical loads on human proximal femora placed in a physiological position corresponding to monopodal stance. Until now boundary conditions of the finite elements models of the femur corresponded to the experimental conditions reflecting a monopodal support.[10–12] Indeed, in this case failure occurs before the fall. However, these conditions *in vivo* do not reflect the conditions of fracture of the femur which occur following a fall.[43] The second phase of this study would be to carry out tests of lateral quasi-static choc.

The model cannot be completely validated because experimentally an elastomer was put between the bone and the device. To improve these results, the solution was to hang some resin with the head bone and scan the system after having positioned the resin. This will allow a model to be more realistic of the experiment results. An analysis of the thickness of the compact bone at failure will be interesting but a geometrical analysis cannot be developed because we do not have access to the scan after failure. After the analysis, it will be interesting to film the failure with a rapid camera and have a better comparison with the beginning of the failure. Finally, a 3D measure of the load will allow validation of the loading conditions more precisely.

Specific orientations were determined from 3D CT scans giving reconstructed 3D images of each femur. The description of bone density and geometry CT scans were used to develop finite element models like Schileo *et al.*[18] The results obtained showed the existence of two groups of fracture profiles. The first group consisted of femora which had sustained subcapital fractures, and the second one contained femora in which the fractures had occurred in the cervical section. The profiles observed in these experimental tests were similar to those of the nontraumatic fractures often observed *in vivo*, mainly in the case of osteoporotic fractures. The failure loads measured in the present experiments (597 ± 252 daN) were comparable to those recorded by Lochmüller (2002) under vertical loading conditions (442 ± 168 daN in men and 291 ± 93 daN in women) and Cody *et al.*[10] when the loading was applied to the femoral head with a 25° frontal inclination (992 ± 322 daN). Ota *et al.*[17] also obtained comparable results with a nonspecified femoral orientation (840 daN).

Among the failure load values obtained on the basis of numerical results using the three failure criteria, those obtained with the Tsai–Wu criterion correlated strongly with the experimental failure load than those based on the Hill and von Mises criteria (Fig. 5). The standard error of the predicted failure load values showed

a lower dispersion with the Tsai–Wu criterion (626 ± 271 daN) than with the Hill (650 ± 299 daN) and von Mises criteria (938 ± 565 daN).

In this study, the main cortical orthotropic direction was assumed to be the neck axis, while the main cortical orthotropic direction was expressed in terms of the Harvesian system.[13] In addition, cancellous bone was assumed to be an isotropic material, although it is known to show large-scale anisotropy,[44] which is subject to great variability, depending on the trabecular density and the orientation. Further modeling studies on the orthotropic behavior of bone based on a more physiological description of the orientation might help to improve the accuracy of finite element model predictions.

This study is different from others as it shows the importance of considering a principal axis (see Table 1). This improves the failure results in comparison with isotropic behavior and Von Mises studies. Moreover, considering the difference between the tension and compression strength of cortical bone improves proximal femur failure predictions, as established in studies by Cezayirlioglu *et al.*[31] on cortical bone samples under combined loading conditions. This finding suggests that the accuracy of failure predictions may depend on the assumed failure mode, and on whether the heterogeneous and orthotropic behavior of bone is taken into account. In spite of the good correlation observed between the predictions based on the von Mises criterion and the experimental results, the failure load values calculated with this method were overestimated. In the experimental tests, femora 1, 2, 3 and 4 sustained a subcapital fracture. In this region, the shear stress is the predominant load. This may explain why all the failure criteria give quite accurate failure load estimates. Only the von Mises criterion overestimated the failure load in femur 3. This overestimation may have been due to numerical dispersion.

5. Conclusion

In conclusion, the tests described above were performed on human personalized specimens. The experimental results obtained were used to check the validity of the finite element simulations. These were based on a numerical study performed on specific finite element models, which were directly generated from CT scan images. An accurate 3D reconstruction of the bone was therefore performed directly from CT scans, making it possible to assign material properties corresponding to the grey level densities observed in the CT scan data to each mesh element. The finite element model was developed and failure loads were predicted based on the beforementioned three failure criteria.

The fracture location differed between these experiments and the finite element models: in the models, it depended on the failure theory used. The Hill and von Mises criteria predicted that the failure would be located in the subcapital section, whereas the Tsai–Wu predicted that it would occur in the subcapital region in the case of femora which had sustained subcapital rupture in the experimental tests, and in the cervical region in the case of those which had sustained cervical fracture.

The present study on nine human proximal femora may open the way to further researches on parameters such as frame orientation, the orthotropic behavior of bone, interactions between the various ways of loading and failure predictions. Further tests using a triaxal load are now required in which the orthotropic behavior and asymmetric strength are taken into account with a view to obtaining more accurate assessments of bone fragility.

Acknowledgments

The authors would like to thank Dr. T. LeCorroller (LaTimone Hospital, Marseille) for providing the specimens and carrying out the CT scan acquisitions, and F. Mazerolle (LMA) for his participation in the mechanical tests.

References

1. Ford CM, Keaveny TM, Hayes WC, The effect of impact direction on the structural capacity of the proximal femur during falls, *J Bone Miner Res* **11**:377–383, 1996.
2. Hayes WC, Myers ER, Morris JN, Gerhart TN, Yett HS, Lipsitz LA, Impact near the hip dominates fracture risk in elderly nursing home residents who fall, *Calcif Tissue Int* **52**:192–198, 1993.
3. Hayes WC, Myers ER, Rovinovitch SN, Van Den Kroonenberg A, Courtney AC, McMahon TA, Etiology and prevention of age related hip fractures, *Bone* **18**:77S–86S, 1996.
4. Nevitt MC, Cummings SR, Type of fall and risk of hip and wrist fractures: The study of osteoporotic fractures, *J Am Geriatr Soc* **41**:1226–1234, 1993.
5. Keyak JH, Kaneko TS, Tehranzadeh J, Skinner HB, Predicting proximal femoral strength using structural engineering models, *Clin Orthop Relat Res* 219–228, 2005.
6. Lotz JC, Cheal EJ, Hayes WC, Fracture prediction for the proximal femur using finite element models: Part I-linear analysis, *J Biomech Eng* **113**:353–360, 1991.
7. Lotz JC, Cheal EJ, Hayes WC, Fracture prediction for the proximal femur using finite element models: Part II-nonlinear analysis, *J Biomech Eng* **113**:361–365, 1991.
8. Ramaniraka NA, Rakotomanana LR, Leyvraz PF, The fixation of the cemented femoral component: Effects of stem stiffness, cement thickness and roughness of the cement bone surface, *J Bone Joint Surg Br* **82**:297–303, 2000.
9. Weinans H, Sumner DR, Igloria R, Natarajan RN, Sensitivity of periprosthetic stress-shielding to load and the bone density-modulus relationship in subject-specific finite element models, *J Biomech* **33**:809–817, 2000.
10. Cody DD, Gross GJ, Hou FJ, Spencer HJ, Goldstein SA, Fyhriea DP, Femoral strength is better predicted by finite element models than QCT and DXA, *J Biomech* **32**(10):1013–1020, 1999.
11. Kaufer H, Matthews LS, Sonstegard D, Stable fixation of the intertrochanteric fracture, *J Bone Joint Surg* **56A**:899–907, 1974.
12. Lang TF, Keyak JH, Heitz MW, Augat P, Lu Y, Mathur A, Genant HK, Volumetric quantitative computed tomography of the proximal femur; precision and relation to bone strength, *Bone* **21**:101–108, 1997.
13. Baca V, Horak Z, Mikulenka P, Dzupa V, Comparison of an inhomogeneous orthotropic and isotropic material models used for Fe analyses, *Med Eng Phys* 2008, in press.

14. Wirtz DC, Schiffers N, Pandorf T, Radermacher K, Weichert D, Forst R, Critical evaluation of known bone material properties to realize anisotropic FE simulation of the proximal femur, *J Biomech* **33**:1325–1330, 2000.
15. Wirtz DC, Pandorf T, Portheine F, Radermacher K, Schiffers N, Prescher A, Weichert D, Niethard FU, Concept and development of an orthotropic FE model of the proximal femur, *J Biomech* **36**:289–293, 2003.
16. Cristofolini L, Juszczyk M, Martelli S, Taddei F, Viceconti M, *In vitro* replication of spontaneous fractures of the proximal human femur, *J Biomech* **40**:2837–2845, 2007.
17. Ota T, Yamamoto I, Morita R, Fracture simulation of the femoral bone using the finite-element method: How a fracture initiates and proceeds, *J Bone Miner Metab* **17**:108–112, 1999.
18. Schileo E, Dall'Ara E, Taddei F, Malandrino A, Schotkamp T, Baleani M, Viceconti M, An accurate estimation of bone density improves the accuracy of subject-specific finite element models, *J Biomech* **41**:2483–2491, 2008.
19. Yosibash Z, Padan R, Joskowicz L, Milgrom C, A ct-based high-order finite element analysis of the human proximal femur compared to *in-vitro* experiments, *J Biomech Eng* **129**:297–309, 2007.
20. Lengsfeld M, Schmitt J, Alter P, Kaminsky J, Leppek R, Comparison of geometry-based and ct voxel-based finite element modelling and experimental validation, *Med Eng Phys* **20**:515–522, 1998.
21. Lotz JC, Cheal EJ, Hayes WC, Stress distributions within the proximal femur during gait and falls: Implications for osteoporotic fracture, *Osteoporos Int* **5**:252–261, 1995.
22. Van Rietbergen B, Huiskes R, Eckstein F, Ruegsegger P, Trabecular bone tissue strains in the healthy and osteoporotic human femur, *J Bone Miner Res* **18**:1781–1788, 2003.
23. Bessho M, Ohnishi I, Okazaki H, Sato W, Kominami H, Matsunaga S, Nakamura K, Prediction of the strength and fracture location of the femoral neck by ct-based finite-element method: A preliminary study on patients with hip fracture, *J Orthop Sci* **9**:545–550, 2004.
24. Couteau B, Hobatho M, Darmana R, Brignola J, Arlaud J, Finite element modelling of the vibrational behavior of the human femur using ct-based individualized geometrical and material properties, *J Biomech* **31**:383–386, 1998.
25. Duchemin L, Mitton D, Jolivet E, Bousson V, Laredo JD, Skalli W, An anatomical subject-specific FE-model for hip fracture load prediction, *Comput Methods Biomech Biomed Eng* **11**:105–111, 2008.
26. Keyak JH, Falkinstein Y, Comparison of *in situ* and *in vitro* ct scan-based finite element model predictions of proximal femoral fracture load, *Med Eng Phys* **25**:781–787, 2003.
27. Keyak JH, Meagher JM, Skinner HB, Mote CDJ, Automated three-dimensional finite element modelling of bone: a new method, *J Biomed Eng* **12**:389–397, 1990.
28. Liang Peng L, Jing B, Xiaoli Z, Yongxin Z, Comparison of isotropic and orthotropic material property assignments on femoral finite element models under two loading conditions, *Med Eng Phys* **28**:227–233, 2006.
29. Keyak JH, Rossi SA, Jones KA, Skinner HB, Prediction of femoral fracture load using automated finite element modelling, *J Biomech* **31**:125–133, 1998.
30. Schileo E, Taddei F, Cristofolini L, Viceconti M, Subject-specific finite element models implementing a maximum principal strain criterion are able to estimate failure risk and fracture location on human femurs tested *in vitro*, *J Biomech* **41**:356–367, 2008.
31. Cezayirlioglu H, Bahniuk E, Davy DT, Heiple KG, Anisotropic yield behavior of bone under combined axial force and torque, *J Biomech* **18**:61–69, 1985.

32. Helgason B, Perilli E, Schileo E, Taddei F, Brynjólfsson S, Viceconti M, Mathematical relationships between bone density and mechanical properties: A literature review, *Clin Biomech* **23**:135–146, 2008.
33. Pithioux M, Lois de comportement et modèles de rupture des os long, Université d'Aix Marseille II, 2000 (in French).
34. Bessho M, Ohnishi I, Matsuyama J, Matsumoto T, Imai K, Nakamura K, Prediction of strength and strain of the proximal femur by a ct-based finite element method, *J Biomech* **40**:1745–1753, 2007.
35. Keyak JH, Rossi SA, Prediction of femoral fracture load using finite element models: An examination of stress- and strain-based failure theories, *J Biomech* **33**:209–214, 2000.
36. Yoshida H, Faust A, Wilckens J, Kitagawa M, Fetto J, Chao EY, Three-dimensional dynamic hip contact area and pressure distribution during activities of daily living, *J Biomech* **39**:1996–2004, 2006.
37. Viceconti M, Bellingeri L, Cristofolini L, Toni A, A comparative study on different methods of automatic mesh generation of human femurs, *Med Eng Phys* **20**:1–10, 1998.
38. Katz JL, Meunier A, The elastic anisotropy of bone, *J Biomech* **20**:1063–1070, 1987.
39. Reilly DT, Burstein AH, The elastic and ultimate properties of compact bone tissue, *J Biomech* **8**:393–405, 1975.
40. Ashman RB, Cowin SC, Van Buskirk WC, Rice JC, A continuous wave technique for the measurement of the elastic properties of cortical bone, *J Biomech* **17**:349–361, 1984.
41. Reilly DT, Burstein AH, Review article, The mechanical properties of cortical bone, *J Bone Joint Surg Am* **56**:1001–1022, 1974.
42. Echaabi J, Trochu F, Gauvin R, Review of failure criteria of fibrous composite materials, *Polym Compos* **17**:786–798, 1996.
43. Cummings SR, Melton LJ, Epidemiology and outcomes of osteoporotic fractures, *Lancet* **359**(9319):1761–1767, 2002.
44. Brown TD, Ferguson ABJ, Mechanical property distributions in the cancellous bone of the human proximal femur, *Acta Orthop Scand* **51**:429–437, 1980.
45. Black J, Hastings G (eds.), *Handbook of Biomaterial Properties*, Chapman & Hall, 1998.
46. Taylor WR, Roland E, Ploeg H, Hertig D, Klabunde R, Warner MD, Hobatho MC, Rakotomanana L, Clift SE, Determination of orthotropic bone elastic constants using FEA and modal analysis, *J Biomech* **35**, 2002.